

Gas system Upgrade for the BaBar IFR detector at SLAC

S. Foulkes^a, J.W. Gary^a, B.C. Shen^a, K. Wang^a, R. Boyce^b,
R. Messner^b, P. Stiles^b, N. Sinev^c, H. R. Band^d,

^a*University of California, Riverside, CA, 92521 USA*

^b*Stanford Linear Accelerator Center, Menlo Park, CA 94025, USA*

^c*University of Oregon, Eugene, OR 97403, USA*

^d*University of Wisconsin, Madison, WI 53706, USA*

Abstract

A new gas distribution and monitoring system was installed as part of an upgrade of the forward endcap muon detection system (IFR) of the BaBar detector at SLAC. Over 300 gas circuits are controlled and monitored. The return gas flow is monitored by digital bubblers which use photo-gate electronics to count the bubbling rate. The rates are monitored in real time and recorded in a history database allowing studies of flow rate versus chamber performance.

Key words: gas system, BABAR

PACS: 29.90+r

1 Introduction

The BaBar detector [1], operating at the PEP-II storage ring of the Stanford Linear Accelerator Center (SLAC) since 1999, was built for the study of CP violations in systems of B hadrons. An important consideration in this program is the accurate identification of muons and neutral hadrons. In BaBar, this identification is performed using the Instrumented Flux Return (IFR) detector, a system of Resistive Plate Chambers (RPCs) inserted into gaps between the steel layers forming the return path for the magnetic field. During the first years of operation, many RPCs exhibited a significant loss of efficiency [1]. Studies of this performance degradation were hindered by the lack of detailed knowledge and control of the gas flow in individual RPC modules.

Work Supported in part by the Department of Energy Contract DE-AC03-76SF00515

An upgrade of the forward endcap IFR in 2002 replaced the original RPCs with RPCs constructed with thinner linseed oil coatings and improved construction and quality control procedures [2]. Additional steel and brass absorber were added to reduce the probability of pion mis-identification and to shield against machine backgrounds. To achieve better control and monitoring of the gas flow into the new RPCs, new gas distribution units were designed, built, and installed. New return bubblers were built which electronically counted the bubble rate of the gas flow returning from the RPCs. The bubbler design was patterned after a similar application implemented for the BELLE detector at KEK [3] with changes designed to improve the reliability and ease of maintenance. In this article, we describe these improvements and the first year of operation of the gas system.

2 GAS System Overview

The IFR gas system [1] is an open system. Mixed gas is produced from tanks of argon, freon, and isobutane and distributed via low pressure manifolds to gas distribution boxes mounted on the detector. After passing through a RPC gas volume (typically 2-3 RPC modules connected in series), the gas flow is measured by return bubblers before being vented to atmosphere. Flow rates vary from 3-8 volume changes per day depending on the type of chamber and expected background exposure.

The BaBar RPCs operate with a gas mixture of 61.2% argon, 34.4% freon 134A, and 4.4% isobutane. The three gas components are mixed using MKS mass-flow controllers. The gas mixture is stored in a 760 liter tank from where it is supplied to the detector at a rate of approximately 12.5 liters/min at a pressure of 5.5 psig. At the detector, a regulator reduces the pressure to 3 inches of water (0.108 psig). A valve manifold divides the flow and distributes gas via 12.7 mm diameter copper tubes to 23 distribution boxes (Sect. 4) located at various points around the IFR. Each distribution box supplies gas to 16 RPC channels via 6.4 mm diameter plastic PTFE tubes at flow rates between 10 and 100 cc/min.

After passing through the RPCs, the return gas is sent to digital bubblers (Sect. 5) which measure the flow rate. The differential ECL signals from the digital bubblers are transmitted by ribbon cables to the VME scalars in the BaBar electronics house. The scalars are read every 2 minutes via EPICS and stored in the BaBar database.

3 Design

Several aspects of the original gas system caused operational difficulties. Individual gas flows were set by uncalibrated needle valves and monitored by visual bubblers. In an attempt to keep the gas lines as short as possible, the input and output units were often mounted in widely separated locations on the detector. The input impedance of the needle valves was low, such that large changes to a channel's flow affected other channels within the same box. Changing the flow of a channel typically required several adjustments. Most importantly, since the visual bubblers were inside the radiation area, no flow information was available without access to the detector. During data-taking such accesses were infrequent and of limited duration. A system was needed so that both the input and output gas flows of each chamber were well measured. Only modest accuracy was required as it was not expected that 20% changes in the gas flow would measurably effect RPC performance.

The gas system upgrade mounted the new distribution boxes and return bubblers in standard racks in a few accessible central locations. The distribution boxes contain flowmeters for each RPC. The bubble rate in each return line is digitized and sent to electronic scalars. These changes required longer gas lines to and from the RPCs, but at the low flows used in the IFR introduced no significant pressure drop. Standard chassis parts were used as much as possible. The units were designed to be interchangeable so that malfunctioning units could be easily replaced during a short access. The photogates were glued onto a plastic front window which could be removed with minimal disturbance to the rest of the unit. Significant variations in the photogate response were observed during tests¹ of prototype systems. It was necessary to provide several adjustable parameters per channel to ensure that uniform signal shapes were achieved.

4 Gas Distribution Boxes

The function of the rack mountable distribution box is threefold: (1) to divide the gas flow into 16 channels, (2) to provide a means to control the flow rate in each channel, and (3) to provide protection against excessive gas pressure. Each distribution box consists of a manifold, two pressure relief bubbler chambers, 16 flow meters, and the associated plastic tubes and feed-through connectors as shown in Fig.1. The gas flow is split into channels by an aluminum manifold. The flow in each channel is regulated by a Dwyer Instru-

¹ We thank Bill Sands and Dan Marlow of Princeton University for providing BELLE prototypes.

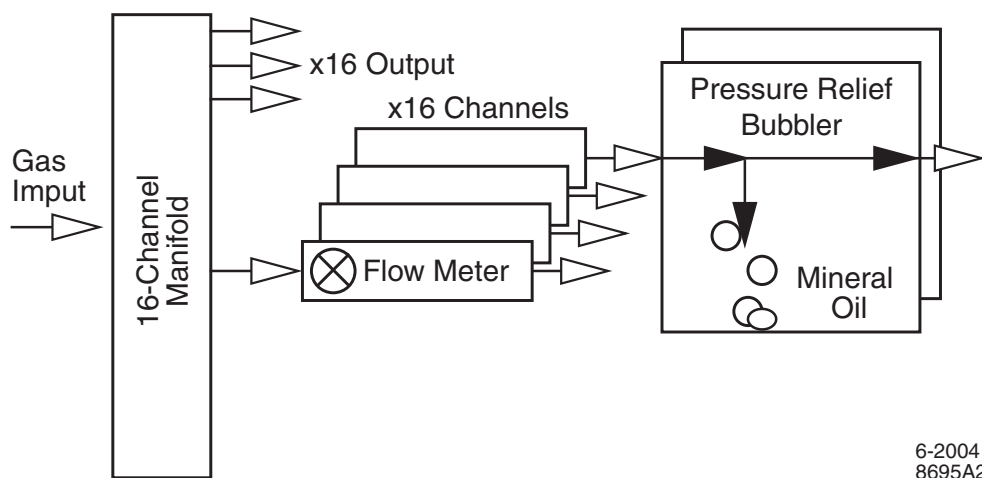


Fig. 1. Schematic diagram of a distribution box.

ments RMA-150-SSV flow meter with an adjustable flow rate of up to 50 or 100 cc/min full scale. The output of each flow meter is connected to a pressure relief bubbler and the RPC. At gas pressures greater than ≈ 1 cm of oil, the relief bubbler allows gas to escape by bubbling through the oil. A photograph of the gas distribution box is shown in Fig. 2.

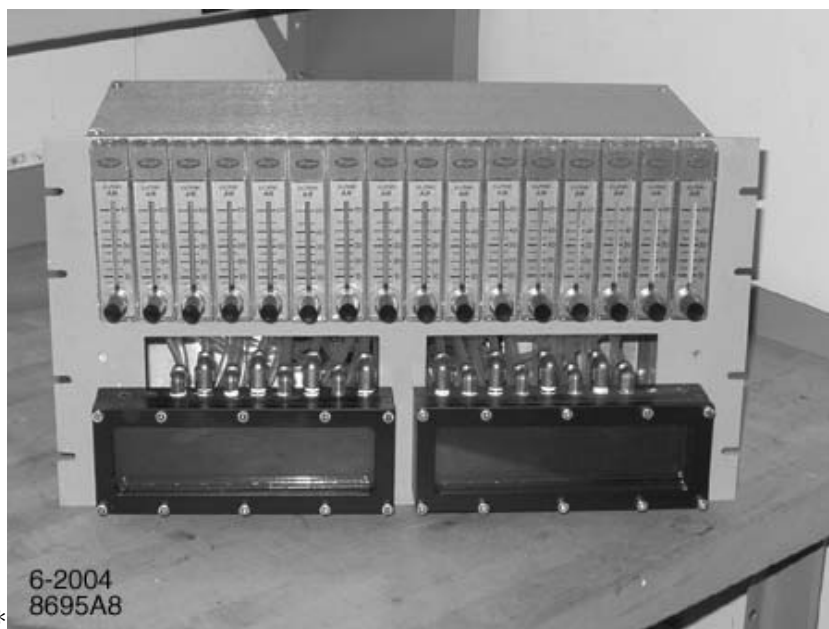


Fig. 2. Photograph of a distribution box. The two pressure relief bubbler chambers (bottom) and 16 flow meters (top) are visible.

5 Digital Bubblers

After exiting the RPCs, the return gas enters the digital bubblers. A schematic diagram of a digital bubbler circuit is shown in Fig. 3a. Gas enters a bubbler chamber containing Dow-Corning 704 diffusion pump fluid through a 3 mm orifice. Bubbles formed by the gas are constricted to pass through a Fairchild H22A1 photo-gate circuit immersed in the fluid. The gas pressure inside the RPCs depends primarily on the back pressure set by the ≈ 7 mm depth of the fluid.

The photo-gate electronics circuit is shown in Fig. 3b. The photo-gate has two components: a LED and a photo-transistor. The intensity of infrared light emitted by the LED can be adjusted using the variable resistor, R_1 accessible from the front panel. The variable load resistance, R_2 , is typically set to $5\text{ k}\Omega$. In the absence of a bubble, most of the LED light reaches the photo-transistor, causing current to flow through R_2 . The resultant output voltage, V_{out} (see Fig. 3b), is about 0.3 V . When a bubble traverses the photo-gate, light from the LED is refracted, reducing the amount of light reaching the photo-transistor such that V_{out} increases to about 2 V or more. V_{out} forms the input to a Fairchild Semiconductor LM339N comparator with a threshold typically set to 1 V . A bubble passing through the photo-gate therefore generates a signal from the comparator. The comparator signal is generated in positive TTL logic, which is then converted to negative MECL using a Motorola MC10124P translator chip.

In our design, R_1 can be adjusted for each channel from the front panel of the

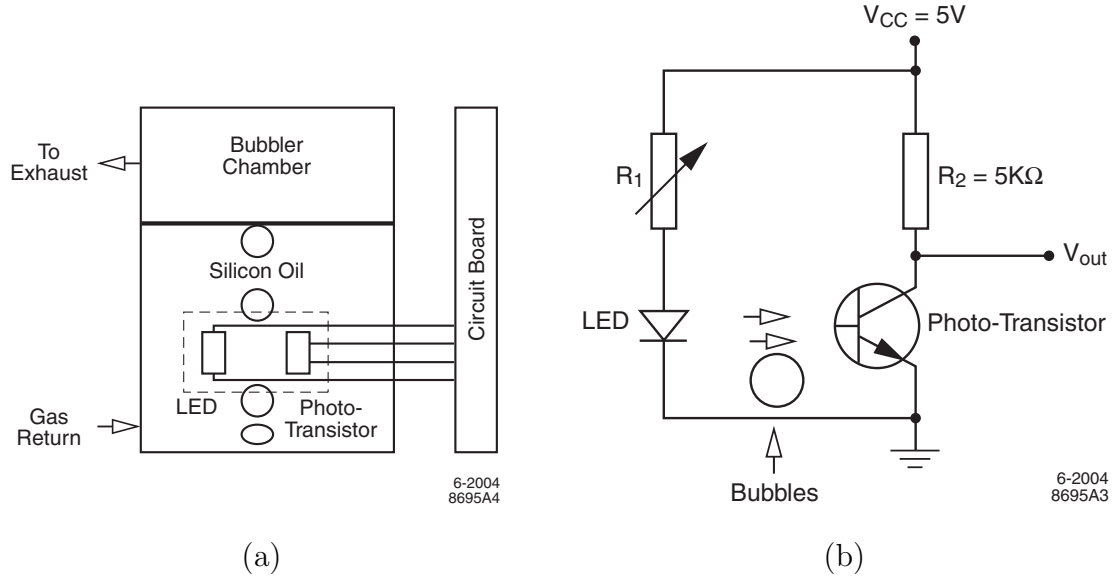


Fig. 3. (a) Schematic diagram of a digital bubbler circuit; (b) digital bubbler electronics circuit diagram.

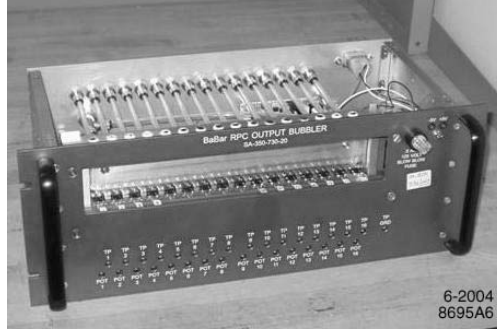


Fig. 4. Photograph of a digital bubbler. The photogates can be seen through the plexiglas panel.

digital bubbler crate. There are also test points on the front panel allowing V_{out} to be monitored for each channel.

Each digital bubbler unit has 16 channels and is rack mountable. A photograph is shown in Fig. 4. The bubbler chamber is constructed from aluminum, with a plexiglas cover sealed with an O-ring. The leads from the photo-gates pass through small holes in the plexiglas and are soldered to a small circuit board. The holes for the leads are then sealed with epoxy. The cover, photogates, and circuit board were attached to the main electronics board by ribbon cable, facilitating replacement of bad photogates or front covers without disassembly of the entire unit.

5.1 Photo-gate signal characteristics

The signals produced by the photo-gates can be directly examined using the test points on the front panel of the digital bubbler crates. Fig. 5a shows a normal signal, corresponding to three bubbles. The initial peak in the signal is due to the scattering of light by the top surface of the bubble. The central valley is the result of reduced scattering from the center of the bubble. The trailing peak is due to the bottom surface of the bubble. If the intensity of the LED is increased, the signal size decreases. In addition, the voltage difference between the peaks and the central valley becomes larger. If the minimum voltage in the central valley drops below the comparator threshold, e.g. because of diurnal variations in the temperature or other instabilities (see below), a bubble can generate two comparator pulses rather than one. It is therefore important to adjust the signal strength to ensure that the minimum voltage level in the valley remains safely above 1 V, taking into consideration the operating conditions of the experiment.

The signal strength from the photo-gate can be increased by decreasing the LED intensity. If the LED intensity becomes too small, the baseline level,

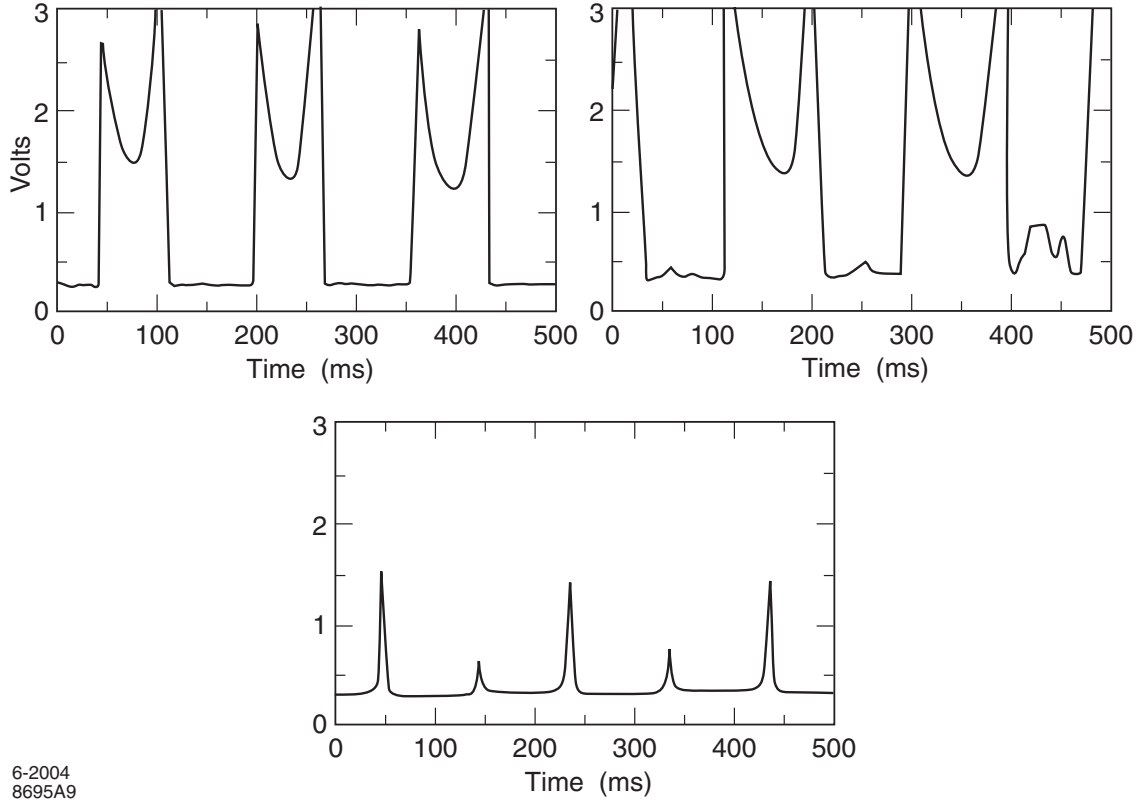


Fig. 5. (a) A normal signal from a photo-gate, corresponding to three bubbles; (b) example of a signal with an unstable baseline; (c) example of a signal in which one of the two peaks associated with the transit of a bubble has dropped below the comparator threshold of 1 V. The ordinate scale of the oscilloscope is in all cases 0.5 V per division.

corresponding to the photo-gate output when no bubble is present, can become unstable, however, as shown in Fig. 5b.

5.2 Photo-gate Instabilities

Using the same commercial mineral oil for the digital bubblers that we use for the relief bubblers of the distribution boxes (Sect. 4), we found the photo-gate signals to be unstable over the operating temperature range of BaBar (20–32 C). For example, photo-gates adjusted to produce a normal signal at the upper end of the temperature range tended to develop an unstable baseline at lower temperatures, while photo-gates adjusted to produce a normal signal at the lower end of the range tended to drop below the 1 V comparator threshold at higher temperatures. Another problem was that 10-15% of the channels demonstrated instabilities even when held at constant temperature. The signals would spontaneously alternate from normal behavior as shown in Fig. 5a to a signal in which one or both peaks was below the comparator threshold

as illustrated in Fig. 5c, with a time period which varied from several minutes to about an hour. Visual examination of the mineral oil revealed that small bubbles of diameter 0.1 mm or less, generated through froth, tended to become suspended in the oil, especially at the lower temperatures. We surmised that some of these froth bubbles could become trapped in small indentations inside the photo-gate assemblies (thus affecting the LED light collected by the photo-transistor), for periods consistent with the observed instabilities, providing a plausible explanation for this behavior.

We tested several different fluids to determine their effect on the photo-gate performance: mineral oil, Leybold HE-175 diffusion pump fluid, Dow-Corning 705 diffusion pump fluid, and Dow-Corning 704 diffusion pump fluid. Of these fluids, only the Dow-Corning 704 fluid produced a stable signal over the desired temperature range. We also observed that the number of froth bubbles suspended in the Dow-Corning 704 fluid at low temperatures was much reduced compared to mineral oil, and that the instabilities described in the previous paragraph were also much reduced. We therefore selected Dow-Corning 704 fluid for use in the digital bubblers.

5.3 Calibration data

To calibrate the digital bubblers, it is necessary to determine the relationship between the bubble rate (from the photo-gate signals) and the gas flow rate. Calibration tests were conducted using Dwyer RMA-150-SSV flow meters, Porter A-125-3, and Gilmont 65 mm meters. For these tests, the output from the flow meters was connected directly to the digital bubblers using approximately 1 m of 6.4 mm diameter tubing. All calibration tests were conducted using compressed air. The tests were based on 48 digital bubbler channels. The temperature of the bubblers was maintained at approximately 29 C using a thermostatically controlled heater.

The results are shown in Fig. 6. It is seen that the dependence of the bubbler rate on the flow rate is not quite linear, with a flattening of the curve as the flow rate increases. This flattening of the calibration curve is consistent with the onset of saturation effects, i.e. the device is limited by how many bubbles per unit time interval can physically pass through the photogate assembly. Nonetheless, it is clear from Fig. 6 that the digital bubblers provide a means to determine the gas flow up to the highest rate tested: 220 cc/min. We note that the flow rates of gas exiting the BaBar RPCs generally lie between 10 and 50 cc/min. corresponding to about 100 to 400 bubbles per minute. We also note that, in our application, the bubblers are primarily used to detect relative changes in the flow of a given channel, and to verify that gas is flowing to all channels, rather than to provide absolute flow measurements.

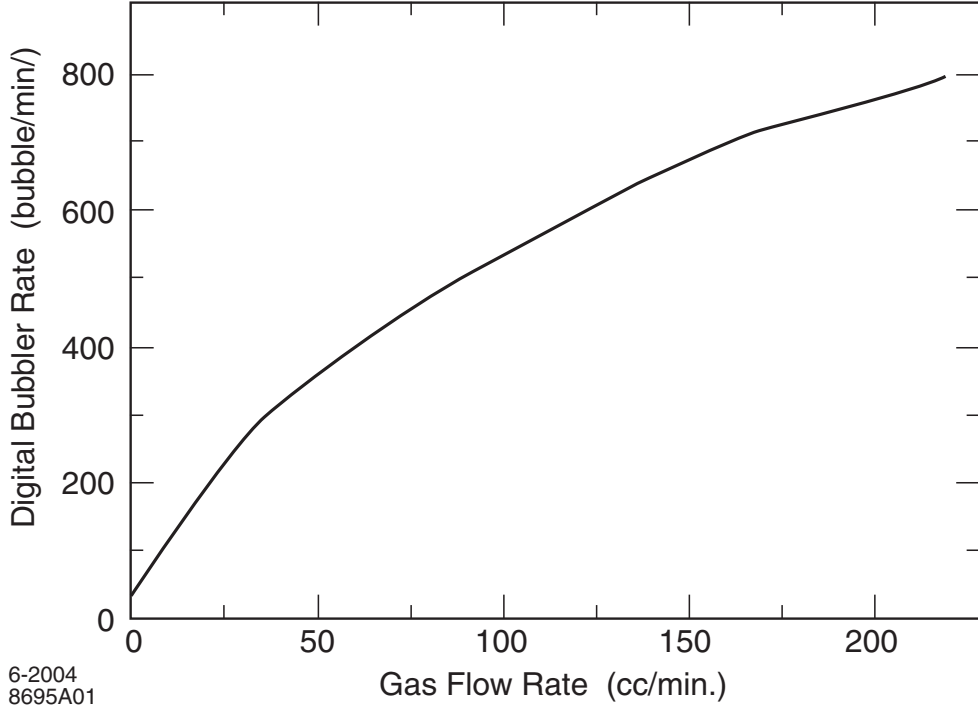


Fig. 6. Digital bubbler calibration curve, averaged over 48 channels.

The barrel RPCs are scheduled to be replaced by Limited Streamer Tubes (LSTs) in 2004 and 2005. The LST system is expected to require a higher gas flow than the RPCs, from about 90 to 120 cc/min. Fig. 6 demonstrates that the digital bubblers will function properly at these higher flow rates, and we intend to incorporate the current digital bubblers into the LST gas system.

5.4 *Temperature dependence*

To study the temperature dependence of our results, the calibration tests were repeated for temperatures between 18° – 38° C. Constant flow rates of either 30 or 45 cc/min were used for these tests. The bubble rates for constant gas flow were found to depend linearly on temperature, with higher bubble rates as the temperature was increased (because the bubbler fluid becomes less viscous as it is heated). Over the operating temperature range of BaBar, the bubble rates were observed to vary by about 10%. This variation is sufficiently small that no correction is applied to the calibration results. We note that the analogous variation observed when mineral oil is used in the digital bubblers, rather than Dow-Corning 704 fluid, is 23%.

5.5 *Stability Tests*

The stability of the bubblers was studied at various flow rates. Bubble rates were recorded every 10 minutes over a four hour period while the flow rate and temperature were kept constant. For flow rates below about 160 cc/min, the bubble rates were observed to be quite stable, with a maximum fluctuation of 2%. For higher flow rates, fluctuations up to about 5% were observed.

6 **Data Acquisition**

The differential ECL signals generated by the digital bubblers were connected by ribbon cable to STRUCK 7201 VME scalars located in the main electronics house. To obtain stable readings of the bubble rate several thousand counts were accumulated for each measurement. Since the bubble rates were typically low (≤ 3 counts per second) this required an integration time of several minutes. A “sliding average” method was developed. The scalars were read every 30 seconds and saved into a circular buffer holding 5 minutes of data per channel. Every new measurement replaced the oldest data in the buffer. The average of the buffer contents contained the necessary statistics yet followed changes in flow rates with better accuracy since it was updated more frequently than measurements using a fixed integration time.

These average bubble rates per channel were available in the online EPICS control software and were recorded into the BaBar conditions database. Every day, web accessible plots showing the previous month’s history were updated. An example of these plots is shown in Fig. 7.

7 **Operational Performance**

New distribution boxes and digital bubblers were installed on the forward endcap and belt layers of the IFR in October 2002, and on the barrel, backward endcap (digital bubblers only) and cylindrical RPC in July 2003. Due to budgetary constraints, new distribution boxes were not installed on the backward endcap, which continues to be supplied using the original system.

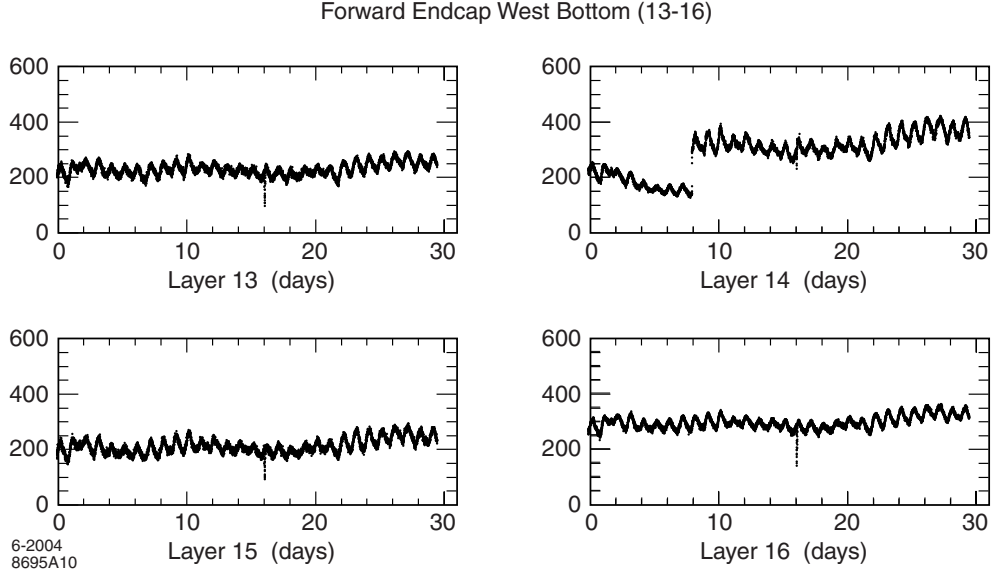


Fig. 7. The bubble rate (bubbles/minute) for 8 channels of the forward endcap are shown for March 2004. Diurnal temperature variations in the detector hall cause the observed oscillations in the recorded rate. The flow in Layer 14 was decreasing in time until the flowmeter was readjusted during an access.

7.1 Distribution Box

The distribution boxes have performed well, allowing rapid adjustments of the flow to each individual RPC. The only significant problem has been that some of the Dwyer meters ($\approx 20\%$) were either very difficult to set or unstable in their flow setting. Most of these meters were identified and replaced during construction and installation. Upon disassembly, many of the unstable meters were found to have had grease from the internal O-rings on the flow control pins. After cleaning, most of these meters appeared to function normally and were placed back into service. In some cases, the threads on the control pins were either too tight or too loose to provide a stable flow, and these meters were discarded.

A few flowmeters developed problems during normal operations. On six occasions, the flow in one of the 272 Dwyer meters did not recover after a gas pressure outage. The bead inside the meter appeared to be stuck at the bottom of the meter. These problems were resolved by either tapping on the meter, temporarily increasing the flow, or cleaning the meter. Occasionally the flow in a channel was observed to decrease with time as shown in Fig. 7 (Layer 14). The flows were restored by readjusting the flowmeter during an access.

If the gas flow is shut off for an extended period of time, the tubes connecting the distribution boxes and digital bubblers to the RPCs must be disconnected. Otherwise, changes in temperature and atmospheric pressure can create a

negative pressure within the RPCs and cause fluid from the distribution boxes or digital bubblers to be drawn into the tubes. This generally creates a large enough back pressure to prevent flow to the RPCs once the gas supply is restored.

7.2 *Digital Bubbler Performance*

Prior to changing from mineral oil to Dow-Corning 704 fluid, we observed periodic rapid fluctuations in the bubble rates without an apparent commensurate change in the flow. This is believed to be a result of the signal instabilities described in Sect. 5.1. Since changing to Dow-Corning 704 fluid, we have not observed this effect.

One significant design flaw has surfaced during the first year. Nearly 1/4 of the bubbler front plexiglass windows have developed cracks around the mounting screw holes leading to oil leaks. The windows are held in place against a rubber O-ring by 16 6-32 inch panhead screws without washers. The first generation windows will be replaced with polycarbonate windows this summer. An aluminum bar will distribute the pressure from the screws more evenly than before, hopefully preventing future problems.

An in-situ comparison was made between the nominal input flow provided by the flowmeters and the outflow measured by the recorded bubble rates channel by channel. In the absence of leaks, the correlation between the measurements demonstrates the accuracy of the overall system. The data are shown in Fig. 8 for the forward endcap and compared to the calibration curve (with air) from Fig. 6. On average the outflow is $\approx 25\%$ lower than expected.

8 Summary

A new gas system for the muon detection system (IFR) of the BaBar detector at SLAC, allowing electronic monitoring of the gas flow rate in each channel, has been described. The principal electronic element of this system is a photo-gate, consisting of an infrared emitting LED and a photo-transistor. The photo-gate is immersed in a bubbler chamber with diffusion pump fluid. Gas exiting an IFR channel forms bubbles in the fluid. The bubbles transit between the LED and photo-transistor, interrupting the light and allowing the bubble rate to be digitized. Calibration studies determine that the digitized bubble rate provides a good measure of the gas flow rate in the detector for flow rates up to at least 220 cc/min. The new gas system has been installed and is performing well, providing important capabilities for monitoring the

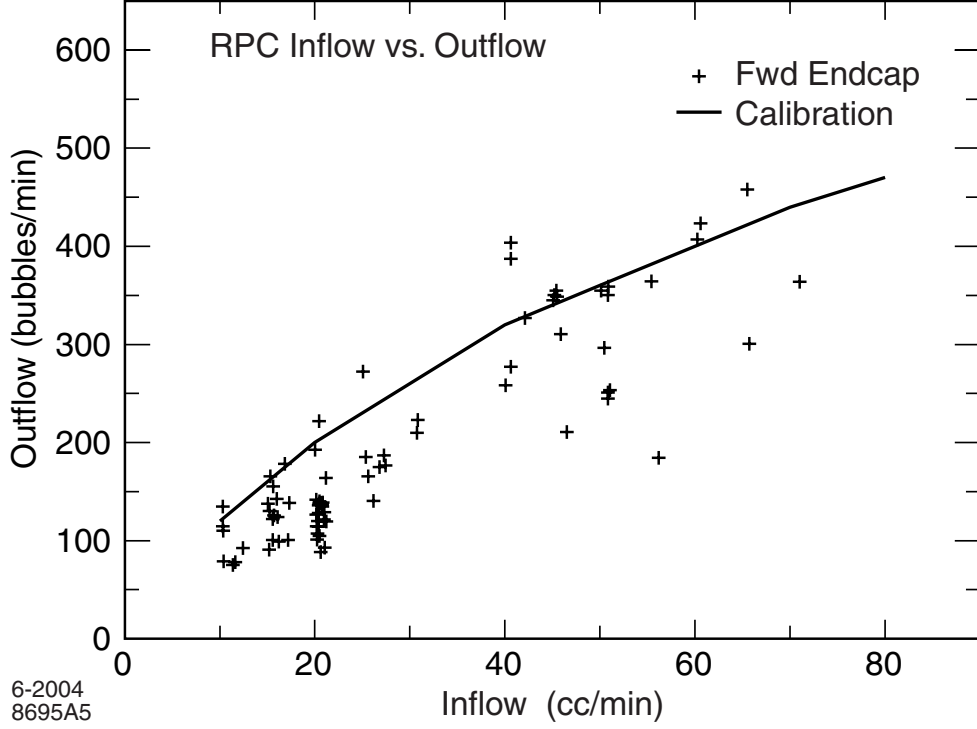


Fig. 8. The bubble rate (bubbles/sec) plotted against the flowmeter reading for all forward endcap RPCs which bubble at the output bubbler. The correlation expected from the calibration data is shown as the red line.

operation of the detector.

9 Acknowledgments

We thank Anglia Little for assistance during calibration tests, and the SLAC and INFN technicians who aided in installation. This work has been supported by the US Department of Energy.

References

- [1] BaBar Collab., B. Aubert et al., Nucl. Instr. Meth. A479 (2002) 1.
- [2] “BaBar Forward Endcap Upgrade” F. Anulli et al., submitted to Nucl. Instr. Meth.
- [3] M. Ahart et al., KEK BELLE Note 135.